CONTINUUM GYROKINETIC SIMULATIONS OF NSTX SOL TURBULENCE WITH SHEATH-LIMITED MODEL GEOMETRIES

A. Hakim[1], E.L. Shi[2,3], T.N. Bernard[4], M. Francisquez[5], G.W. Hammett[1], F. Jenko[6,4], N.R. Mandell[3], Q. Pan [7], T. Stoltzfus-Dueck[1], D. Told[6]

[1] Princeton Plasma Physics Laboratory, Princeton, NJ 08543-0451, USA, [2] Lawrence Livermore National Laboratory, Livermore, California 94550, USA, [3] Princeton University, Princeton, NJ 08544, USA, [4] University of Texas, Austin, TX 78712, USA, [5] Dartmouth College, Hanover, NH 03755, USA, [6] Max Planck Institute for Plasma Physics, Garching, Germany, [7] MIT Plasma Science and Fusion Center, Cambridge, MA 02139, USA

Corresponding Author: ahakim@pppl.gov

Abstract:

We describe results obtained from Gkeyll, a full-F continuum gyrokinetic code, designed to study turbulence in the edge region of fusion devices. The edge region is computationally very challenging, requiring robust algorithms that can handle large amplitude fluctuations and stable interactions with sheath boundary conditions. Results of turbulence in a scrape-off layer (SOL) for NSTX-type parameters with a model magnetic geometry have been obtained. Key physics of SOL turbulence, such as drive by toroidal bad curvature and steep gradients and interactions with a model sheath boundary condition are included. This allows us to perform parameter scans and physics studies, such as the physics of heat flux width on the divertor plate, and the amplitude and intermittency of SOL turbulence. Initial results find that the heat flux narrows as the connection length is made shorter (the poloidal field becomes stronger). To validate the code, we have studied turbulence in the straight-field LAPD device at UCLA and the Helimak device at the University of Texas. We will also describe the extension of the GENE gyrokinetic code to be full-F, and initial GENE simulations for LAPD.

1 INTRODUCTION

An outstanding challenge in fusion research is developing a quantitative understanding of the edge plasma, its interaction with material walls, and its impact on fusion performance. A lack of quantitative understanding of the edge is a road-block to optimization of fusion performance, and design of reactor-grade burning plasma machines. Although relatively narrow, the edge plasma, however, is very challenging computationally, with the need to handle a wide range of scales, large amplitude fluctuations near the beta limit, stable interactions with a sheath model, and complex atomic and surface physics.

To attack this challenging problem, we are developing a complex computational tool, `Gkeyll`, which will allow quantitative predictions of edge physics that we plan to test against experiments, and some initial experimentally relevant simulations are shown here. The `Gkeyll` code employs novel versions of high-order Discontinuous Galerkin (DG) algorithms, extensively developed in the computational fluid dynamics community[6]. Our algorithms conserve energy exactly for Hamiltonian systems in the continuous time limit. The use of robust higher-order schemes can significantly help with the computational challenges of the edge region. Higher order DG methods, which have a sub-cell representation of the solution allow significant flexibility in creating algorithms that are robust, yet continue to preserve important conserved quantities (density and energy) as well as maintain physical bounds on solution (positivity of the distribution function).

Gkeyll has recently been used to demonstrate the first successful simulations using continuum algorithms of bad-curvature-driven turbulence on open field lines with sheath boundary conditions. The continuum code GENE has done similar simulations in straight field configurations. We give highlights of these Gkeyll and GENE results here. The XGC code, using PIC algorithms, is at present the only gyrokinetic turbulence code able to handle open and closed field line regions simultaneously.

This paper is organized as follows. First, we describe the algorithms implemented in `Gkeyll` followed by a linear benchmark in which we compute the growth rate of ETG modes and compare them to analytical results. Next, we show results from various physics studies carried out with `Gkeyll`. We have performed simulations of turbulence in the straight-field LAPD device[22], and found fluctuation amplitude and intermittency levels quali-

tatively similar to that found in experiments and previous fluid calculations. Simulations of biasing experiments on LAPD[19] that drive strong sheared flows, find that turbulence is suppressed as observed in experiments[23]. We recently[23, 21] extended these straight-field simulations to a curved helical field (a toroidal field plus a vertical field), and carried out simulations of this helical model SOL for NSTX-type parameters. We give some highlights of these model SOL simulations here.

The GENE continuum gyrokinetic code has been widely used to study turbulence in the main core region of tokamaks and stellarators. The global version has recently been extended to include the parallel nonlinearity, making it equivalent to a full-F code, and extended to include sheath boundary conditions. It has been demonstrated on a 1D ELM heat pulse problem for JET[17], finding similar results as Gkeyll[20]. The full 3x2v version of the code has recently simulated LAPD turbulence[18], also finding similar results to Gkeyll[22].

In our initial SOL simulations, we have modeled the magnetic field as a toroidal field plus a vertical field, which is sufficient for several physics studies. This same geometry can also be used to simulate toroidal devices such as the Helimak, and we show some initial comparisons with experiments.

Areas for future work include implementation of more complex magnetic geometry, extensions to include electromagnetic fluctuations, and some models of atomic physics. While the present work shows the overall feasibility of the continuum approach to simulating plasma edge turbulence and allow initial physics studies, these extensions should allow for more detailed comparisons with experiments on tokamaks and other plasma devices.

2 GYROKINETIC MODEL AND DISCONTINOUS GALERKIN ALGORITHM

`Gkeyll` uses an energy-conserving, mixed discontinuous Galerkin (DG), continuous Galerkin (CG) scheme for the gyrokinetic equations (GK) written as a Hamiltonian evolution equation

$$\frac{\partial f}{\partial t} + \{f, H\} = C[f]. \tag{1}$$

Here $f(t, \mathbf{z})$ is a distribution function, $H(\mathbf{z})$ is the Hamiltonian and $\{g, f\}$ is the Poisson bracket operator, and $C[f]$ is the collision operator. The coordinates $\mathbf{z} = (z^1, \ldots, z^N)$ label the N-dimensional phase-space in which the distribution function evolves. Defining the phase-space velocity vector $\boldsymbol{\alpha} = (\dot{z}^1, \ldots, \dot{z}^N)$, where the characteristic speeds are determined from $\dot{z}^i = \{z^i, H\}$, allows rewriting Eq. (1), on use of the Liouville theorem on phase-space incompressibility, $\nabla \cdot (\mathcal{J}\boldsymbol{\alpha}) = 0$, where ∇ is the gradient operator in phase-space, in an explicit conservation law form

$$\frac{\partial}{\partial t}(\mathcal{J} f) + \frac{\partial}{\partial z^i}\left(\mathcal{J}\dot{z}^i f\right) = \mathcal{J} C[f] \tag{2}$$

where $\mathcal{J}$ is the Jacobian of the transform from canonical to (potentially) non-canonical coordinates. Note that if the coordinates are canonical, $\mathcal{J} = 1$. This is the form in which `Gkeyll` evolves the equations.

In this paper we will use a long-wavelength limit of the gyrokinetic model with electrostatic fluctuations. The phase space is five-dimensional ($N = 5$), the Hamiltonian is

$$H = \frac{1}{2} m v_\parallel^2 + \mu B + q\phi \tag{3}$$

and the non-canonical Poisson Bracket operator is

$$\{F, G\} = \frac{\mathbf{B}^*}{m B_\parallel^*} \cdot \left(\nabla F \frac{\partial G}{\partial v_\parallel} - \frac{\partial F}{\partial v_\parallel} \nabla G \right) - \frac{c\hat{\mathsf{b}}}{q B_\parallel^*} \times \nabla F \cdot \nabla G. \tag{4}$$

where $\mathbf{B}^* = \mathbf{B} + (B v_{||}/\Omega) \nabla \times \hat{\mathsf{b}}$ and $B_{||}^* = \hat{\mathsf{b}} \cdot \mathbf{B}^*$. From the Poisson structure one can show that the Jacobian is $\mathcal{J} = m^2 B_\parallel^*$. The potential appearing in the Hamiltonian is determined from the equation of quasi-neutrality, also referred to as the gyrokinetic Poisson equation, which we use in the linearized polarization limit, that is

$$-\nabla \cdot (\epsilon_\perp \nabla_\perp \phi) = \rho_c = \sum_s q \int d^3 v f \tag{5}$$

where $\epsilon_\perp$ is the perpendicular plasma polarization coefficient. In the above we follow some of the notation of [14]. See Sugama [24], Cary and Brizard[5], and Brizard and Hahm[4] for derivation and details of the various terms in these expressions.

Historically, many widely used numerical methods for simulating Hamiltonian systems in plasmas, especially the Vlasov equation, are based on a particle-in-cell[3, 13] (PIC) approach, a class of Lagrangian schemes that introduce macro-particles that move in phase space with the characteristic velocity $\boldsymbol{\alpha}$. Another approach, adopted in our work, is to solve the Hamiltonian equation directly by discretizing it using a continuum Eulerian scheme. In recent years efficient high-order schemes, especially of the discontinuous Galerkin family[7, 8], have become popular for computational fluid dynamics applications[26] and are well suited to application to the phase-space flow described by the gyrokinetic Vlasov equations.

Continuum algorithms, like the one described in this paper, have certain advantages over traditional particle methods. The most obvious one is the elimination of particle noise that can be challenging, in certain parameter regimes, for standard PIC algorithms. Importantly, well designed continuum schemes based on the DG approach, due to flexibility of basis and test functions, can be designed in such a manner that conserved quantities of the continuous system, such as total (fluid plus field) energy and momentum can be exactly or accurately conserved.

To discretize the gyrokinetic equation, we introduce a phase-space mesh $\mathcal{T}$ with cells $K_j \in \mathcal{T}$, $j = 1, \ldots, N$ and introduce the following piecewise polynomial approximation space for the distribution function $f(t, \mathbf{z})$

$$\mathcal{V}_h^p = \{v : v|_K \in \mathbf{P}^p, \forall K \in \mathcal{T}\} \tag{6}$$

where $\mathbf{P}^p$ is (some) space of polynomials. To approximate the Hamiltonian, on the other hand, we introduce the space

$$\mathcal{W}_{0,h}^p = \mathcal{V}_h^p \cap C_0(\mathbf{Z}) \tag{7}$$

where $\mathbf{Z}$ is the phase-space domain. Essentially, we allow the distribution function to be discontinuous, while requiring that the Hamiltonian is in the continuous subset of the space used for the distribution function.

The problem can now be stated as finding $f_h \in \mathcal{V}_h^p$ such that, for all $K_j \in \mathcal{T}$,

$$\int_{K_j} w \frac{\partial f_h}{\partial t}\, d\mathbf{z} + \oint_{\partial K_j} w^- \mathbf{n} \cdot \boldsymbol{\alpha}_h \hat{F}\, dS - \int_{K_j} \nabla w \cdot \boldsymbol{\alpha}_h f_h\, d\mathbf{z} = 0, \tag{8}$$

for all test functions $w \in \mathcal{V}_h^p$. Here, $\mathbf{n}$ is an outward unit vector on the surface of the cell K_j. In this *discrete weak-form*, $\hat{F} = \hat{F}(f_h^-, f_h^+)$ is a numerical flux function. Further, the subscript h indicates the discrete solution and the notation w^- (w^+) indicates that the function is evaluated just inside (outside) on the location on the surface ∂K_j.

The energy conservation properties for Hamiltonian problems in phase-space are indirect, involving integration by parts and field-particle energy exchange, and are not automatic as they are for finite-volume treatments of fluid equations where there is an explicit energy conservation equation. Part of energy conservation in phase-space requires that the discrete scheme satisfy one of the quadratic invariants of the Poisson bracket, i.e. $\int H\{f, H\}\, d\mathbf{z} = 0$, the integration taken over all phase-space. However, total energy conservation (particles plus field) usually requires use of the corresponding field equation, and hence also imposes additional constraints on its solution.

With our schemes and choice of basis functions we can prove that the total number of particles is conserved exactly, and energy (particles plus field) is conserved exactly in the continuous time limit. That is, spatial scheme conserves total energy exactly:

$$\frac{\partial}{\partial t} \int_\Omega \left(\mathcal{E}_h(\mathbf{x}, t) + \frac{\epsilon_\perp}{8\pi} |\nabla_\perp \phi_h(\mathbf{x}, t)|^2 \right)\, d\mathbf{x} = 0 \tag{9}$$

where $\mathcal{E}_h$ is the discrete particle energy. In addition, we can show that the second Casimir invariant, that is, the L_2 norm of the distribution function, can be conserved with a special choice of numerical fluxes, while it decays monotonically with upwinding.

We have spent significant effort to make our schemes robust, allowing us to obtain reasonably accurate results even with coarse resolution. A particular challenge is to ensure that the distribution function does not become negative. A negative distribution function can cause nonphysical instabilities and also modify the energy content of the simulation adversely. To ensure positivity we have developed a novel scheme in which the moments of the distribution function in each phase-space cell are used to reconstruct a local exponential which is, by definition, positive. The basic idea in a 1D example is the following. A standard DG approach is to expand $f_{\text{lin}}(x, t) = f_0(t) + f_1(t)x$ in piecewise linear basis functions, and ensure that the error projected onto the basis functions is 0, leading to Eq. 8. For a cell domain $x \in [-1, 1]$, strict positivity requires $|f_1|/f_0 < 1$. But we can also interpret Eq. 8 as giving the time evolution of moments $M_0 = \int dx f$ and $M_1 = \int dx f x$. As long as $-1 \leq \langle x \rangle \leq 1$, where $\langle x \rangle = M_1/M_0$, which corresponds to the less restrictive limit $|f_1|/f_0 < 3$, then one can always find an

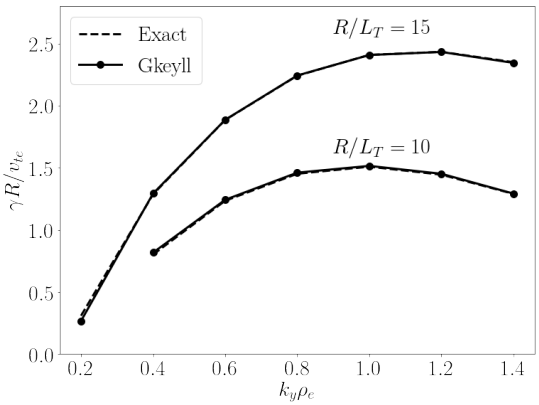

FIG. 1: Linear growth rates for a toroidal ETG problem computed from `Gkeyll` *simulations (solid) compared to analytically obtained values from dispersion relation (dashed) for two different values of R/L_T, with $R/L_n = 0$, $k_\parallel R = 0.5$ and $\tau_e = 1$. The* `Gkeyll` *growth rates compare very well to analytical theory for a broad range of $k_y\rho_e$.*

equivalent positive exponential representation $f_{\exp} = \exp(\beta_0 + \beta_1 x)$ with these same moments. This exponential reconstruction is then used in the update formula for surface fluxes. Combined with flux limiters that cap the particles leaving a phase-space cell in a single time-step, this rigorously ensures that the solution remains positive.

The collision terms are modeled at present using a Lenard-Bernstein operator (LBO). See Shi thesis[23] for details. This operator, although significantly simpler than the full Fokker-Planck operator, contains the basic structure of collisional processes relevant to the edge plasma, that is, a combination of drag and diffusion. The LBO is discretized using a "recovery" based discontinuous Galerkin method[25]. In velocity space, the LBO conserves particles, momentum, and energy. To ensure this property is preserved in a system with spatial variations, we have developed novel DG-based techniques to recover moments consistently with conservation requirements as well as boundary conditions. These will described in a later publication.

3 LINEAR ETG BENCHMARK

To benchmark our code we have performed a large number of tests, comparing code output to analytical or previously published results. In this section we describe a simple, but very useful, ETG linear benchmark that demonstrates the ability of the code to obtain correct linear behavior even when using the full nonlinear code. A simple purely toroidal magnetic field is used, so one can do analytical derivation of the growth rate without solving a ballooning-type eigenvalue problem (this is a local limit of the toroidal ETG instability, for modes localized near $\theta = 0$). With finite $k_{||}$, this problem requires full 3D2V capability, and so tests many code components simultaneously.

To linearize the gyrokinetic Vlasov equation we write $H = H_0 + H_1$ and $f = f_0 + f_1$, where the subscripts 0 and 1 indicate equilibrium and perturbed quantities respectively. (The code remains in full f form, but radial periodic boundary conditions are applied to $f - f_0$, in order to remove the non-periodic linear gradient in f_0.) With this, the Poisson bracket can be linearized as $\{H, f\} = \{H_0, f_1\} + \{H_1, f_0\}$. Combining this with the linearized field equations, and assuming a local limit with kinetic electrons and adiabatic ions, and neglecting FLR corrections except in the polarization density, we obtain the dispersion relation[1, 2]

$$\tau_e + k_\perp^2\rho_e^2 + R_0(x) + R_1(x)\frac{R}{L_n} + R_2(x)\frac{R}{L_T} = 0, \tag{10}$$

with

$$R_0(x) = 1 + i\int_0^\infty d\tau e^{i\tau x}e^{-\tau^2 z_\parallel^2/2(1+2i\tau)}\frac{x}{(1+i\tau)\sqrt{1+2i\tau}} \tag{11}$$

$$R_1(x) = -i\int_0^\infty d\tau e^{i\tau x}e^{-\tau^2 z_\parallel^2/2(1+2i\tau)}\frac{1}{(1+i\tau)\sqrt{1+2i\tau}} \tag{12}$$

$$R_2(x) = i\int_0^\infty d\tau e^{i\tau x}e^{-\tau^2 z_\parallel^2/2(1+2i\tau)}\frac{1}{(1+i\tau)\sqrt{1+2i\tau}}\left(\frac{3}{2} - \frac{1}{1+i\tau} - \frac{1+2i\tau-\tau^2 z_\parallel^2}{2(1+2i\tau)^2}\right) \tag{13}$$

and $\tau_e = T_e/T_i$, $x = \omega/\omega_{de}$, $z_\parallel = k_\parallel v_{te}/\omega_{de}$, and $\omega_{de} = k_y\rho_e v_{te}/R$, with $v_{te} = \sqrt{T_e/m_e}$. Note that unlike in Beer[1], we neglect all FLR corrections (effectively taking $b = 0$ in Beer's equations 2.64-2.66) except for the

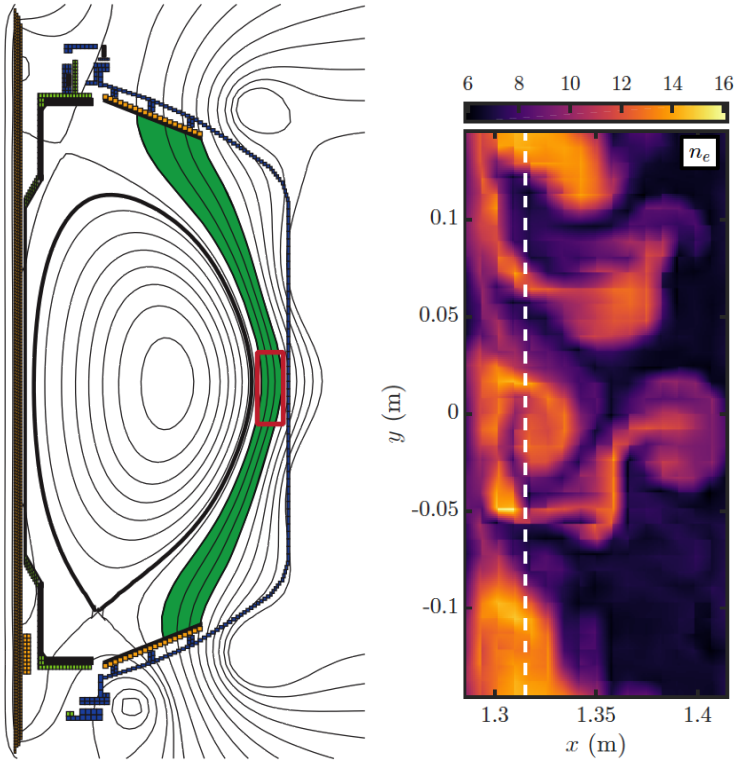

FIG. 2: Left: Cross-section of an MHD equilibrium in NSTX. The SOL region shaded in green illustrates the simulation domain, using a helical model of the SOL magnetic field, with a toroidal plus a vertical magnetic field. The right plot zooms in on the red box. Right: A snapshot of turbulent density fluctuations (in units of $10^{19}/m^3$) near the midplane of the SOL, calculated by the full-F continuum code `Gkeyll`*. (The source is strongly localized around $R = 1.3$ m, left of the white dashed line.) (From [23] and [21].)*

second order FLR correction that gives the polarization density in the quasineutrality equation, which results in the $k_\perp^2 \rho_e^2$ term in Eq. (10). Results are shown in Fig. 1 for two choices of R/L_T, with $R/L_n = 0$, $k_\parallel R = 0.5$ and $\tau_e = 1$. This shows that the numerically computed growth rates from `Gkeyll` simulations agree well with the analytical dispersion relation above.

4 PHYSICS STUDIES ON OPEN FIELD GEOMETRIES

4.1 Turbulence in a model helical SOL geometry for NSTX

Our first turbulence simulations on open field lines were done with straight magnetic fields[22, 23], for parameters typical of the LAPD device. These demonstrated that the algorithms could handle large amplitude fluctuation sufficiently well, that the interactions between the gyrokinetic equations and boundary conditions to model sheaths were stable and physically reasonable, that the predicted turbulence characteristics (fluctuation amplitudes, degree of intermittency, etc.) were qualitatively similar to those observed in LAPD, and thus demonstrated the overall feasibility of a continuum approach to simulating edge turbulence.

Our next step was to extend to curved magnetic fields, which introduce grad B and curvature drifts, and thus the bad curvature drive of toroidal instabilities that can often be quite strong. This allows us to do a simple helical model of the magnetic field in a tokamak SOL. We choose parameters to be comparable to a typical SOL region in NSTX. The simulation domain is like the green SOL region indicated in Fig. 2(a), straightened out to vertical flux surfaces. The simulation domain (using field-aligned coordinates) is a flux tube that follows field lines that start at the bottom divertor plate, go around the torus and eventually hit the top divertor plate.

Fig. 2(b) shows a snapshot of turbulent density fluctuations from the simulation near the midplane, zooming in on the red box in Fig. 2(a). We model the flux of particles and heat from the core of the plasma across the separatrix, and the particle source from ionization of neutrals, as a Maxwellian source of particles near the midplane that is radially highly localized (a Gaussian with $\sigma = 0.5$ cm) around $x = R = 1.30$ m, to the left of the white dotted line in Fig. 2(b), plus a small source (at a rate 0.1 times the peak) that is uniform in x. (This small radially-uniform source also helps prevent the density in the far SOL from getting too small and causing numerical problems. The final density profile including turbulent radial transport is fairly broad compared to this source profile, but future work can study the impact of different source profiles.) The particle fuelling rate and the

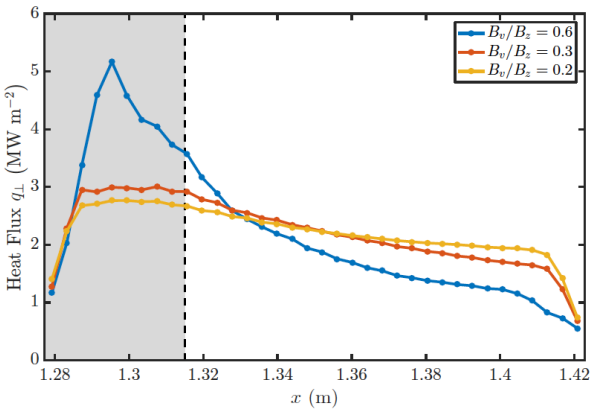

FIG. 3: Profiles of the heat flux to the divertor target plates, for several different values of poloidal (vertical) field B_v, indicating that the heat flux width is narrowest at the highest poloidal field.

temperature of the source were chosen to give a power into the SOL of $P_{\rm sol} = 5.4$ MW, comparable to an NSTX case. The source temperature (74 eV for electrons and ions) was chosen to give a plasma temperature near the left side of the box comparable to what is seen at the separatrix in experiments. (The resulting temperatures from the simulation in the source region were $T_i \sim 50$ eV and $T_e \sim 30$ eV, dropping to much lower temperatures in the far SOL.) For this given $P_{\rm sol}$, this source temperature also turns out to give about the right electron density near the separatrix. Although the source temperature was an adjustable parameter, the shape of the predicted temperature and density profiles are the result of self-consistent balance between the very narrow source, radial broadening by turbulence, and parallel losses to the divertor plate.

The simulations produce turbulence that has characteristics similar to experimental observations. The rms fluctuation levels are largest in the steep gradient region around the white dotted line in Fig. 2(b). Blobs tend to form there and occasionally detach and propagate a large distance radially, giving more intermittent fluctuations in the far SOL, as seen in the figure. If the curvature is turned off and straight field lines are used in the simulation, then the blobs do not propagate very far in the radial direction and the overall turbulence level drops, indicating the importance of the bad curvature drive.

In Fig. 3 we show how the radial profile of the heat flux to the divertor plates varies as the poloidal (i.e., vertical) field varies. We find that the SOL heat flux width narrows as the poloidal field increases. This is qualitatively similar to experimental scalings[9, 11], though the physical mechanism sometimes invoked may differ, since there are no magnetic drifts across flux surfaces in our present geometry. As the poloidal field increases, the connection length from midplane to the divertor plate shortens, which can have a direct stabilizing effect on some instabilities and also shortens the parallel loss time, so turbulence has less time to spread plasma radially before it hits the end plates. We know there are important physical processes that need to be added to the code before we expect quantitatively accurate predictions (such as more complete magnetic geometry, finite-beta magnetic fluctuations, etc.), but it is interesting to see features in the present simulations that are qualitatively similar to experiments. Further details about these helical SOL simulations for NSTX can be found in [23, 21].

4.2 Turbulence in Helimak experiment and experimental validation

We used Gkeyll to simulate the Texas Helimak[10], a simple magnetized torus experiment at the University of Texas at Austin. This device has a toroidal magnetic field ($B_{\rm max} < 0.13$ T), a vertical field, major radius $R = 1.1$ m, plasma half width 0.5 m, and vertical height 2 m. It uses RF heating to make plasmas with densities of order 0.1-1 $\times 10^{17}$/m^3 and electron temperatures of order 5-10 eV, and has an extensive array of probes to measure characteristics of the plasma and turbulence. We do not yet have radiation, charge exchange, or ionization directly in the code, and a large fraction of the input power can be radiated away for the Helimak case under consideration, so we adjusted the power in the source (i.e., the source temperature) to give about the right average electron temperature seen in the experiment. The particle source rate was also chosen to give about the right average density, but this source was taken to be very narrow (since it is concentrated near narrow RF resonance layers), as indicated in Figure 4. The simulation density profile shape, which is determined self-consistently by the turbulence, agrees relatively well with the experimental data, as shown in Fig. 4. It is much broader than the source, so the profile shape indicates that the predicted turbulent transport is about right.

The right part of Figure 4 shows turbulence profiles calculated as the root-mean-square of ion density fluctuations over the local (in R) mean density. Despite differences at larger radii, these levels are closer than those

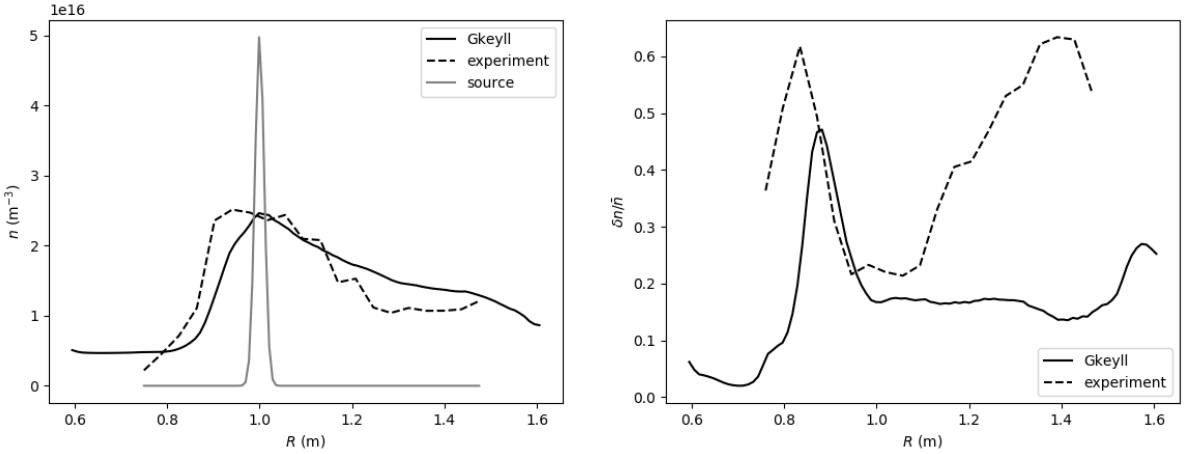

FIG. 4: Left: Helimak ion density steady state profiles from experiment and simulation (Gkeyll), and source profile in the simulation. The simulation predicts about the right density profile shape self-consistently from the turbulent spreading, independent of the narrow particle source. Right: Experimental and simulated profile of the turbulent fluctuation amplitudes, $\delta n_{\rm rms}/n$, for a Helimak case. Despite differences at larger radii, these levels are closer than those achieved in past simulations.

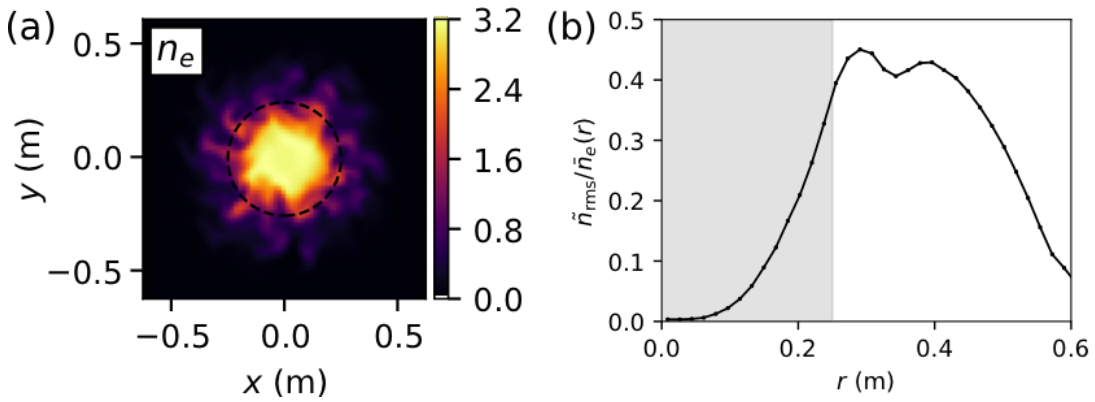

FIG. 5: Results from the GENE simulation of LAPD turbulence. (a) A snapshot of the electron density (in $10^{18}\ m^{-3}$) on the mid-plane in a quasi-steady state. The dashed circle with radius $r = 0.25$ m indicates the edge of the top-hat source. (b) The RMS of the electron density fluctuations as a function of radius, normalized to the local mean density. The shaded area indicates the source region. (This figure is adopted from Fig. 3a and Fig. 6b of Reference[18], reprinted with permission).

achieved with fluid simulations of the Helimak[16]. The predicted electron temperature for the present input power is about 30% low on average compared to the experiment. In future work we can investigate if increasing the source input power (which will raise the temperature) will affect the parallel loss rate and profiles enough to improve the level of agreement in the fluctuation amplitudes at large R.

4.3 Open Field line modelling with GENE

The continuum gyrokinetic GENE code has been under continuous development for two decades or so and widely applied to turbulence studies of the core region of tokamaks and stellarators[15, 12]. To handle unique properties of edge plasmas, including large amplitude fluctuations and plasma-wall interactions in the SOL, the global version of the code was extended[17] to include the $E_{||}$ velocity-space nonlinearity, sheath boundary conditions, and a nonlinear Lenard-Bernstein collision operator, for electrostatic applications. The extended code is equivalent to and can be run as a full-f code. The code employs either traditional or weighted essentially non-oscillatory (WENO) upwind finite-volume methods for the parallel dynamics, finite-differencing for the perpendicular dynamics, and a particle- and energy-conserving finite-volume method for the collisions.

To compare with Gkeyll, a 1D1V code was extracted from the 3D2V GENE code to simulate the parallel transport of a ELM heat pulse from the mid-plane to the divertor target in JET SOL. It was demonstrated that a large sheath potential builds up upon the arrival at the divertor target of suprathermal electrons, confining the bulk electrons with the ions. Consequently, the main ELM heat flux loading occurs on the ion transit time scale.

The heat flux deposited onto the divertor target quantitatively agrees with the `Gkeyll` result[17]. The full 3D2V version of the code has modeled LAPD turbulence driven continuously in time by a density and heat source centered around the axis of the plasma column. In response to the density built up in the top-hat-shape source region, waves and turbulence develop at the source edge with a steep density gradient, resulting in the rotating azimuthal structures that are seen in the Gkeyll simulations and resemble the experiment data from the imaging camera. The strongest density fluctuations (normalized to the local mean density) occur outside of the source edge, and the maximum fluctuations are at the 40% level. This is qualitatively consistent with the experimental data from the Langmuir probe. Overall, we found that the time-averaged profiles and the fluctuation statistics are in qualitative agreement with Gkeyll results and experimental data; detailed comparisons and comments can be found in [18]. Extensions to Gkeyll and GENE to add things such as atomic physics and a more detailed treatment of the electron beam that heats LAPD could be done for more detailed quantitative comparisons with experiments.

ACKNOWLEDGEMENTS

This research was supported by U.S. DOE contract DE-AC02-09CH11466, in part through the DOE SciDAC Partnership for Multiscale Gyrokinetic Turbulence and the Max-Planck/Princeton Center for Plasma Physics.

REFERENCES

[1] M A Beer. *Gyrofluid Models of Turbulent Transport in Tokamaks*. PhD thesis, Princeton University, November 1994.
[2] M. A. Beer and G. W. Hammett. Toroidal gyrofluid equations for simulations of tokamak turbulence. *Physics of Plasmas*, 3:4046–4064, November 1996.
[3] C.K Birdsall and A. B Langdon. *Plasma Physics Via Computer Simulation*. Institute of Physics Publishing, 1990.
[4] A J Brizard and T S Hahm. Foundations of nonlinear gyrokinetic theory. *Reviews of Modern Physics*, 79(2):421–468, April 2007.
[5] John R Cary and Alain J Brizard. Hamiltonian theory of guiding-center motion. *Reviews of Modern Physics*, 81(2):693–738, May 2009.
[6] B Cockburn and C W Shu. Runge–Kutta discontinuous Galerkin methods for convection-dominated problems. *Journal of Scientific Computing*, 16(3):173–261, 2001.
[7] B Cockburn and C W Shu. Runge–Kutta discontinuous Galerkin methods for convection-dominated problems. *Journal of Scientific Computing*, 16(3):173–261, 2001.
[8] B Cockburn and Chi-Wang Shu. The Runge–Kutta Discontinuous Galerkin Method for Conservation Laws V. *Journal of Computational Physics*, 141:199–224, April 1998.
[9] T. Eich, A.W. Leonard, R.A. Pitts, W. Fundamenski, R.J. Goldston, T.K. Gray, A. Herrmann, A. Kirk, A. Kallenbach, O. Kardaun, A.S. Kukushkin, B. LaBombard, R. Maingi, M.A. Makowski, A. Scarabosio, B. Sieglin, J. Terry, A. Thornton, ASDEX Upgrade Team, and JET EFDA Contributors. Scaling of the tokamak near the scrape-off layer H-mode power width and implications for ITER. *Nucl. Fusion*, 53(9):093031, 2013.
[10] K. W. Gentle and H. He. Texas helimak. *Plasma Science and Technology*, 10(3):284, 2008.
[11] R.J. Goldston. Heuristic drift-based model of the power scrape-off width in low-gas-puff h-mode tokamaks. *Nuclear Fusion*, 52(1):013009, 2012.
[12] T. Görler, X. Lapillonne, S. Brunner, T. Dannert, F. Jenko, F. Merz, and D. Told. The global version of the gyrokinetic turbulence code gene. *Journal of Computational Physics*, 230(18):7053 – 7071, 2011.
[13] R.H. Hockney and J.W. Eastwood. *Computer Simulation Using Particles*. Taylor & Francis, 1989.
[14] Y. Idomura, H. Urano, N. Aiba, and S. Tokuda. Study of ion turbulent transport and profile formations using global gyrokinetic full-f Vlasov simulation. *Nucl. Fusion*, 49(6):065029, 2009.
[15] F. Jenko, D. Told, T. Görler, J. Citrin, A. Ban Navarro, C. Bourdelle, S. Brunner, G. Conway, T. Dannert, H. Doerk, D.R. Hatch, J.W. Haverkort, J. Hobirk, G.M.D. Hogeweij, P. Mantica, M.J. Pueschel, O. Sauter, L. Villard, E. Wolfrum, and the ASDEX Upgrade Team. Global and local gyrokinetic simulations of high-performance discharges in view of iter. *Nuclear Fusion*, 53(7):073003, 2013.
[16] B. Li, B. N. Rogers, P. Ricci, and K. W. Gentle. Plasma transport and turbulence in the Helimak: Simulation and experiment. *Phys. Plasmas*, 16(8), 2009.
[17] Q. Pan, D. Told, and F. Jenko. Fully nonlinear δf gyrokinetics for scrape-off layer parallel transport. *Phys. Plasmas*, 23(10):102302, 2016.
[18] Q Pan, D Told, E L Shi, G W Hammett, and F Jenko. Full-f version of GENE for turbulence in open-field-line systems. *Physics of Plasmas*, 25(6):062303–14, June 2018.
[19] D. A. Schaffner, T. A Carter, G. D. Rossi, et al. Modification of turbulent transport with continuous variation of flow shear in the Large Plasma Device. *Phys. Rev. Lett.*, 109:135002, Sep 2012.
[20] E. L. Shi, A. H. Hakim, and G. W. Hammett. A gyrokinetic one-dimensional scrape-off layer model of an edge-localized mode heat pulse. *Phys. Plasmas*, 22(2), 2015.
[21] E. L. Shi, G. W. Hammett, T. Stoltzfus-Dueck, and Hakim A. Full-f gyrokinetic simulation of turbulence in a helical open-field-line plasma. submitted, `https://arxiv.org`, 2018.
[22] E. L. Shi, G. W. Hammett, T. Stoltzfus-Dueck, and A. Hakim. Gyrokinetic continuum simulation of turbulence in a straight open-field-line plasma. *J. Plasma Phys.*, 83:905830304, 2017. https://arxiv.org/abs/1702.03052.
[23] E.L. Shi. *Gyrokinetic Continuum Simulation of Turbulence in Open-Field-Line Plasmas*. PhD thesis, Princeton University, 2017. https://arxiv.org/abs/1708.07283.
[24] H. Sugama. Gyrokinetic field theory. *Phys. Plasmas*, 7(2):466–480, 2000.
[25] Bram van Leer and Shohei Nomura. Discontinuous Galerkin for Diffusion. In *17th AIAA Computational Fluid Dynamics Conference*. American Institute of Aeronautics and Astronautics, 2005. `http://dx.doi.org/10.2514/6.2005-5108`.
[26] P E Vincent and A Jameson. Facilitating the Adoption of Unstructured High-Order Methods Amongst a Wider Community of Fluid Dynamicists. *Mathematical Modelling of Natural Phenomena*, 6(3):97–140, May 2011.